ANALYSIS OF CROSS-PLY LAMINATES WITH PIEZOELECTRIC FIBER-REINFORCED COMPOSITE ACTUATORS USING FOUR-VARIABLE REFINED PLATE THEORY

Jafar Rouzegar, Farhad Abad

Shiraz University of Technology, Department of Mechanical and Aerospace Engineering, Shiraz, Iran

e-mail: rouzegar@sutech.ac.ir

This study presents an analytical solution for cross-ply composite laminates integrated with a piezoelectric fiber-reinforced composite (PFRC) actuator subjected to electromechanical loading using the four-variable refined plate theory. This theory predicts parabolic variation of transverse shear stresses and satisfies the zero traction on the plate surfaces without using the shear correction factor. Using the principle of minimum potential energy, the governing equations for simply supported rectangular plates are extracted and the Navier method is adopted for solution of the equations. The comparison of obtained results with other common plate theories and the exact solution indicates that besides the simplicity of the presented formulation, it is very accurate in analysis of laminated composite plates integrated with PFRC. Also the effects of the thickness ratio, aspect ratio, number of layers, staking sequence and amount of electrostatic loading on the displacements and stresses are investigated and the obtained findings are reported.

Keywords: cross-ply laminates, electromechanical loading, four-variable theory, PFRC actuator

1. Introduction

In the recent decades, piezoelectric materials due to their intrinsic coupled electromechanical properties have been widely used as actuators and sensors in smart structures. Advantages of piezoelectric materials like quick response, large power generation, work at very low temperatures and vacuum compatibility cause these materials are widely utilized in structural engineering, like aerospace, naval, automobile and space structures. A number of attractive piezoelectric materials like PZT, PVDF are available, but these monolithic piezoelectric material have certain limitations like low piezoelectric constants, shape control (due to their weight) and high specific acoustic impedance. To overcome these limitations, usage of piezoelectric fiber-reinforced composite (PFRC) has been an obvious choice (Kumar and Chakraborty, 2009). Malik and Ray (2003) obtained effective piezoelectric coefficients of PFRC using a micromechanical model through the strength of material approach.

Many investigators studied various analyses of composite laminates with embedded or surface bonded piezoelectric layers, acting as sensors and actuators. Wang and Rogers (1991) proposed an analytical solution of simply supported plates with embedded piezoelectric layers using the classical laminated plate theory (CLPT). Mitchell and Reddy (1995) presented a higher order shear deformation theory (HSDT) for composite laminates with a piezoelectric laminate. Ray *et al.* (1993) presented an exact solution for simply supported square composite laminate with embedded piezoelectric layers. Exact and finite element (FE) solutions for analysis of smart structures containing PFRC actuators were proposed by Malik and Ray (2004) and Ray and Malik (2004), respectively. Shiyekar and Kant (2011) presented a higher order shear and normal deformation theory (HOSNT12) for analysis of laminates with PFRC actuators.

A very recently developed shear deformation plate theory is a two-variable refined plate theory that contains only two unknown parameters and satisfies the condition of free stress without using the shear correction factor. This theory was introduced by Shimpi (2002) for isotropic plates and then extended to orthotropic plates by Shimpi and Patel (2006a) and Thai and Kim (2012). Analysis of laminated composite plates was done by Kim *et al.* (2009a) and vibration and buckling studies were performed by Shimpi and Patel (2006b) and Kim *et al.* (2009b), respectively. In the two-variable refined plate theory, the plate middle surface is assumed to be unstrained and, therefore, only the bending effects are considered. In the four-variable refined plate theory, two other parameters regarding in-plane displacements of the plate middle surface are added. This theory was used for free vibrations of FG plates and bending analysis of FG sandwich plates by Benachour *et al.* (2011) and Hamidi *et al.* (2014), respectively. Using this theory, thermal buckling analysis of FG plates was performed by Bouiadjra *et al.* (2012).

In this paper, the four-variable refined plate theory is utilized for analysis of a laminate composite integrated with piezoelectric actuators. Results obtained for various electromechanical loads are compared with already published results. It is observed that the present theory is very simple and accurate for analysis of laminates with PFRC actuators. Also the effect of the thickness ratio, aspect ratio, electrostatic load, and stacking sequence on displacements and stresses are studied.

2.   Theory and formulations

Consider a simply supported rectangular cross-ply laminate of length a, width b integrated with a piezoelectric fiber-reinforced composite (PFRC) layer as shown in Fig. 1. The right-handed Cartesian coordinate system is located at the corner of the middle plane of the plate. Thickness of the elastic substrate is h and thickness of the actuator is t_p where t_p is small compared with h.
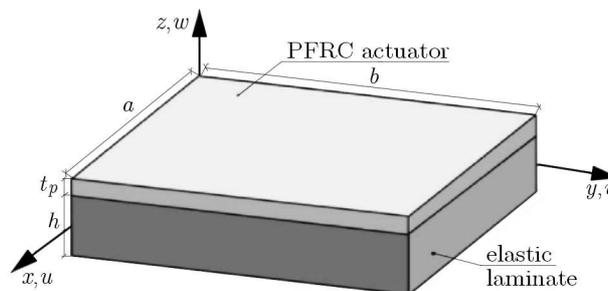

Fig. 1. Geometry of the elastic substrate simply supported along all edges attached with a PFRC actuator at the top

The plate is subjected to electromechanical loading due to the piezoelectric actuator located at the top side. The four-variable refined plate theory is employed for modeling of flexure of the plate.

2.1.   Displacement and strain

According to assumptions of the refined plate theory, the displacement field (u in x-direction, v in y-direction and w in z-direction) is introduced as below (Shimpi, 2002)

$$u(x,y,z) = u_0(x,y) - z\frac{\partial w_b}{\partial x} + z\Big[\frac{1}{4} - \frac{5}{3}\Big(\frac{z}{h}\Big)^2\Big]\frac{\partial w_s}{\partial x}$$

$$v(x,y,z) = v_0(x,y) - z\frac{\partial w_b}{\partial y} + z\Big[\frac{1}{4} - \frac{5}{3}\Big(\frac{z}{h}\Big)^2\Big]\frac{\partial w_s}{\partial y} \tag{2.1}$$

$$w(x,y,z) = w_b(x,y) + w_s(x,y)$$

where u_0 and v_0 are the in-plane displacements of the mid-plane in the x and y direction, and w_b and w_s are the bending and shear component of the transverse displacement, respectively. The strain-displacement relationships are given by

$$\begin{Bmatrix} \varepsilon_x \\ \varepsilon_y \\ \varepsilon_{xy} \end{Bmatrix} = \begin{Bmatrix} \varepsilon_x^0 \\ \varepsilon_y^0 \\ \gamma_{xy}^0 \end{Bmatrix} + \begin{Bmatrix} \chi_x^b \\ \chi_y^b \\ \chi_{xy}^b \end{Bmatrix} + f\begin{Bmatrix} \chi_x^s \\ \chi_y^s \\ \chi_{xy}^s \end{Bmatrix} \qquad \begin{Bmatrix} \gamma_{yz} \\ \gamma_{xz} \end{Bmatrix} = \begin{Bmatrix} \gamma_{yz}^s \\ \gamma_{xz}^s \end{Bmatrix} \qquad \varepsilon_z = 0 \tag{2.2}$$

where

$$\begin{Bmatrix} \varepsilon_x^0 \\ \varepsilon_y^0 \\ \gamma_{xy}^0 \end{Bmatrix} = \begin{Bmatrix} \dfrac{\partial u_0}{\partial x} \\ \dfrac{\partial v_0}{\partial y} \\ \dfrac{\partial u_0}{\partial y} + \dfrac{\partial v_0}{\partial x} \end{Bmatrix} \qquad \begin{Bmatrix} \chi_x^b \\ \chi_y^b \\ \chi_{xy}^b \end{Bmatrix} = \begin{Bmatrix} \dfrac{\partial^2 w_b}{\partial x^2} \\ \dfrac{\partial^2 w_b}{\partial y^2} \\ -2\dfrac{\partial^2 w_b}{\partial x}\partial y \end{Bmatrix}$$

$$\begin{Bmatrix} \chi_x^s \\ \chi_y^s \\ \chi_{xy}^s \end{Bmatrix} = \begin{Bmatrix} -\dfrac{\partial^2 w_s}{\partial x^2} \\ -\dfrac{\partial^2 w_s}{\partial y^2} \\ -2\dfrac{\partial^2 w_s}{\partial x}\partial y \end{Bmatrix} \qquad \begin{Bmatrix} \gamma_{yz}^s \\ \gamma_{xz}^s \end{Bmatrix} = \begin{Bmatrix} \dfrac{\partial w_s}{\partial y} \\ \dfrac{\partial w_s}{\partial x} \end{Bmatrix} \tag{2.3}$$

$$f = -\frac{1}{4}z + \frac{5}{3}z\Big(\frac{z}{h}\Big)^2 \qquad g = \frac{5}{4} - 5\Big(\frac{z}{h}\Big)^2$$

2.2. Constitutive equations

Elastic and electric fields for a single piezoelectric layer are coupled by the following linear constitutive equations

$$\boldsymbol{\sigma} = \mathbf{Q}\boldsymbol{\varepsilon} - \mathbf{e}\mathbf{E} \qquad \mathbf{D} = \mathbf{e}^{\mathrm{T}}\boldsymbol{\varepsilon} + \boldsymbol{\eta}\mathbf{E} \tag{2.4}$$

where $\mathbf{Q}$ is the stress-reduced stiffness, $\mathbf{e}$ is the piezoelectric constants matrix, $\boldsymbol{\eta}$ is the dielectric constant matrix, $\mathbf{E}$ is the electric field intensity vector and $(\boldsymbol{\sigma}, \boldsymbol{\varepsilon})$ are stress and strain tensors. The electric field owing to the variation in stresses (the direct piezoelectric effect) is assumed to be insignificant compared with the applied electric field. This assumption has been utilized by several researchers in literature, see Shiyekar and Kant (2011), Kapuria *et al.* (1997), Reddy (1999) and Tauchert (1992). The coefficients Qij are known as functions of the engineering constants in the principal material directions

$$Q_{11} = \frac{E_1}{1 - \nu_{12}\nu_{21}} \qquad Q_{12} = \frac{\nu_{12}E_2}{1 - \nu_{12}\nu_{21}} \qquad Q_{22} = \frac{E_2}{1 - \nu_{12}\nu_{21}}$$

$$Q_{44} = G_{23} \qquad Q_{55} = G_{13} \qquad Q_{66} = G_{12} \tag{2.5}$$

The effective piezoelectric constant matrix $\mathbf{e}$ and the dielectric matrix $\boldsymbol{\eta}$ for the PFRC layer are given as

$$\mathbf{e} = \begin{bmatrix} 0 & 0 & e_{31} \\ 0 & 0 & e_{32} \\ 0 & 0 & e_{33} \\ 0 & 0 & 0 \\ 0 & e_{24} & 0 \\ e_{15} & 0 & 0 \end{bmatrix} \qquad \boldsymbol{\eta} = \begin{bmatrix} \eta_{11} & 0 & 0 \\ 0 & \eta_{22} & 0 \\ 0 & 0 & \eta_{33} \end{bmatrix} \tag{2.6}$$

The electric field $\mathbf{E}$ is derivable from an electrostatic potential ψ

$$E_i = -\psi_{,i} \qquad i = 1, 2, 3 \tag{2.7}$$

Since the laminate is made of several orthotropic laminas whose material axes are oriented arbitrarily respect to the laminate coordinates, the constitutive equations of each lamina must be transformed to the laminate coordinates (x, y and z in Fig. 1)

$$\begin{Bmatrix} \sigma_x \\ \sigma_y \\ \sigma_{xy} \end{Bmatrix} = \begin{bmatrix} \overline{Q}_{11} & \overline{Q}_{12} & \overline{Q}_{16} \\ \overline{Q}_{12} & \overline{Q}_{22} & \overline{Q}_{26} \\ \overline{Q}_{16} & \overline{Q}_{26} & \overline{Q}_{66} \end{bmatrix} \begin{Bmatrix} \varepsilon_x \\ \varepsilon_y \\ \varepsilon_{xy} \end{Bmatrix} - \begin{bmatrix} 0 & 0 & \overline{e}_{31} \\ 0 & 0 & \overline{e}_{32} \\ 0 & 0 & \overline{e}_{36} \end{bmatrix} \begin{Bmatrix} E_x \\ E_y \\ E_z \end{Bmatrix}$$

$$\begin{Bmatrix} \sigma_{yz} \\ \sigma_{xz} \end{Bmatrix} = \begin{bmatrix} \overline{Q}_{44} & \overline{Q}_{45} \\ \overline{Q}_{45} & \overline{Q}_{55} \end{bmatrix} \begin{Bmatrix} \gamma_{yz} \\ \gamma_{xz} \end{Bmatrix} - \begin{bmatrix} \overline{e}_{14} & \overline{e}_{24} & 0 \\ \overline{e}_{15} & \overline{e}_{25} & 0 \end{bmatrix} \begin{Bmatrix} E_x \\ E_y \\ E_z \end{Bmatrix} \tag{2.8}$$

where

$$\begin{bmatrix} \overline{Q}_{11} & \overline{Q}_{12} & \overline{Q}_{16} \\ \overline{Q}_{12} & \overline{Q}_{22} & \overline{Q}_{26} \\ \overline{Q}_{16} & \overline{Q}_{26} & \overline{Q}_{66} \end{bmatrix} = \mathbf{T}_1^{-1} \begin{bmatrix} Q_{11} & Q_{12} & 0 \\ Q_{12} & Q_{22} & 0 \\ 0 & 0 & Q_{66} \end{bmatrix} \mathbf{R}\mathbf{T}_1\mathbf{R}^{-1}$$

$$\begin{bmatrix} \overline{Q}_{44} & \overline{Q}_{45} \\ \overline{Q}_{45} & \overline{Q}_{55} \end{bmatrix} = \mathbf{T}_2 \begin{bmatrix} Q_{44} & 0 \\ 0 & Q_{55} \end{bmatrix} \mathbf{T}_2^{\mathrm{T}}$$

$$\mathbf{T}_1 = \begin{bmatrix} \cos^2\theta & \sin^2\theta & 2\cos\theta\sin\theta \\ \sin^2\theta & \cos^2\theta & -2\cos\theta\sin\theta \\ -\cos\theta\sin\theta & \cos\theta\sin\theta & \cos^2\theta - \sin^2\theta \end{bmatrix} \tag{2.9}$$

$$\mathbf{R} = \begin{bmatrix} 1 & 0 & 0 \\ 0 & 1 & 0 \\ 0 & 0 & 2 \end{bmatrix} \qquad \mathbf{T}_2 = \begin{bmatrix} \cos\theta & \sin\theta \\ -\sin\theta & \cos\theta \end{bmatrix}$$

and the transformed piezoelectric moduli $\overline{e}_{ij}$ are

$$\begin{aligned}
\overline{e}_{31} &= e_{31}\cos^2\theta + e_{32}\sin^2\theta & \overline{e}_{32} &= e_{31}\sin^2\theta + e_{32}\cos^2\theta \\
\overline{e}_{33} &= e_{33} & \overline{e}_{36} &= (e_{31} - e_{32})\sin\theta\cos\theta \\
\overline{e}_{14} &= (e_{15} - e_{24})\sin\theta\cos\theta & \overline{e}_{24} &= e_{24}\cos^2\theta + e_{15}\sin^2\theta \\
\overline{e}_{15} &= e_{15}\cos^2\theta + e_{24}\sin^2\theta & \overline{e}_{25} &= (e_{15} - e_{24})\sin\theta\cos\theta
\end{aligned} \tag{2.10}$$

The first set of Eqs. (2.4) can be divided into the elastic (e) and piezoelectric (p) stress component

$$\boldsymbol{\sigma} = \boldsymbol{\sigma}^e - \boldsymbol{\sigma}^p \tag{2.11}$$

2.3. Governing equation

The governing equations will be obtained using the principle of minimum potential energy

$$\delta(U + V) = 0 \tag{2.12}$$

where the potential energy of external loads is given by

$$V = -\int_A q(w_b + w_s)\, dx\, dy \tag{2.13}$$

and the strain energy of the laminate is determined as

$$U = \frac{1}{2}\int_v \sigma_{ij}\varepsilon_{ij}\, dv = \frac{1}{2}\int_v (\sigma_x\varepsilon_x + \sigma_y\varepsilon_y + \sigma_{xy}\gamma_{xy} + \sigma_{yz}\gamma_{yz} + \sigma_{xz}\gamma_{xz})\, dv \tag{2.14}$$

Equation (2.15) is obtained by substituting Eq. (2.2) into Eq. (2.14)

$$
\begin{aligned}
U = \frac{1}{2}\int_A & (N_x^e\varepsilon_x^0 - N_x^p\varepsilon_x^0 + N_y^e\varepsilon_y^0 - N_y^p\varepsilon_y^0 + N_{xy}^e\gamma_{xy}^0 - N_{xy}^p\gamma_{xy}^0 + M_x^{e,b}\chi_x^b - M_x^{p,b}\chi_x^b \\
& + M_y^{e,b}\chi_y^b - M_y^{p,b}\chi_y^b + M_{xy}^{e,b}\chi_{xy}^b - M_{xy}^{p,b}\chi_{xy}^b + M_x^{e,s}\chi_x^s - M_x^{p,s}\chi_x^s + M_y^{e,s}\chi_y^s \\
& - M_y^{p,s}\chi_y^s + M_{xy}^{e,s}\chi_{xy}^s - M_{xy}^{p,s}\chi_{xy}^s + Q_{yz}^e\gamma_{yz}^s - Q_{yz}^p\gamma_{yz}^s + Q_{xz}^e\gamma_{xz}^s - Q_{xz}^p\gamma_{yz}^s)\, dx\, dy
\end{aligned}
\tag{2.15}
$$

in which the elastic stress resultants and piezoelectric stress resultants are defined in Eqs. (2.16) and Eqs. (2.17), repectively

$$(N_x^e, N_y^e, N_{xy}^e) = \sum_{k=1}^{N}\int_{Z_K}^{Z_{K+1}} (\sigma_x^e, \sigma_y^e, \sigma_{xy}^e)\, dz \qquad (Q_{yz}^e, Q_{xz}^e) = \sum_{k=1}^{N}\int_{Z_K}^{Z_{K+1}} (\sigma_{yz}^e, \sigma_{xz}^e)\, dz$$

$$(M_x^{e,b}, M_y^{e,b}, M_{xy}^{e,b}) = \sum_{k=1}^{N}\int_{Z_K}^{Z_{K+1}} (\sigma_x^e, \sigma_y^e, \sigma_{xy}^e)z\, dz \tag{2.16}$$

$$(M_x^{e,s}, M_y^{e,s}, M_{xy}^{e,s}) = \sum_{k=1}^{N}\int_{Z_K}^{Z_{K+1}} (\sigma_x^e, \sigma_y^e, \sigma_{xy}^e)f\, dz$$

and

$$(N_x^p, N_y^p, N_{xy}^p) = \sum_{k=1}^{N}\int_{Z_K}^{Z_{K+1}} (\sigma_x^p, \sigma_y^p, \sigma_{xy}^p)\, dz = \sum_{k=1}^{N}\int_{Z_K}^{Z_{K+1}} (\overline{e}_{31}^k, \overline{e}_{32}^k, \overline{e}_{36}^k)E_z^k\, dz$$

$$(M_x^{p,b}, M_y^{p,b}, M_{xy}^{p,b}) = \sum_{k=1}^{N}\int_{Z_K}^{Z_{K+1}} (\sigma_x^p, \sigma_y^p, \sigma_{xy}^p)z\, dz = \sum_{k=1}^{N}\int_{Z_K}^{Z_{K+1}} (\overline{e}_{31}^k, \overline{e}_{32}^k, \overline{e}_{36}^k)E_z^k z\, dz$$

$$(M_x^{p,s}, M_y^{p,s}, M_{xy}^{p,s}) = \sum_{k=1}^{N}\int_{Z_K}^{Z_{K+1}} (\sigma_x^p, \sigma_y^p, \sigma_{xy}^p)f\, dz = \sum_{k=1}^{N}\int_{Z_K}^{Z_{K+1}} (\overline{e}_{31}^k, \overline{e}_{32}^k, \overline{e}_{36}^k)E_z^k f\, dz \tag{2.17}$$

$$\begin{Bmatrix} Q_{yz}^p \\ Q_{xz}^p \end{Bmatrix} = \sum_{k=1}^{N}\int_{Z_k}^{Z_{k+1}} \begin{bmatrix} \overline{e}_{14} & \overline{e}_{24} & 0 \\ \overline{e}_{151} & \overline{e}_{25} & 0 \end{bmatrix}^k \mathbf{E}\, dz$$

Substituting Eqs. (2.8) into Eqs. (2.16) and integrating through the plate thickness, the elastic stress resultants are given as

$$\left\{ \begin{array}{c} \left\{ \begin{array}{c} N_x^e \\ N_y^e \\ N_{xy}^e \end{array} \right\} \\ \left\{ \begin{array}{c} M_x^{e,b} \\ M_y^{e,b} \\ M_{xy}^{e,b} \end{array} \right\} \\ \left\{ \begin{array}{c} M_x^{e,s} \\ M_y^{e,s} \\ M_{xy}^{e,s} \end{array} \right\} \end{array} \right\} = \left[\begin{array}{ccc} \left[\begin{array}{ccc} A_{11} & A_{12} & A_{16} \\ A_{12} & A_{22} & A_{26} \\ A_{16} & A_{26} & A_{66} \end{array} \right] & \left[\begin{array}{ccc} C_{11} & C_{12} & C_{16} \\ C_{12} & C_{22} & C_{26} \\ C_{16} & C_{26} & C_{66} \end{array} \right] & \left[\begin{array}{ccc} E_{11} & E_{12} & E_{16} \\ E_{12} & E_{22} & E_{26} \\ E_{16} & E_{26} & E_{66} \end{array} \right] \\ \left[\begin{array}{ccc} C_{11} & C_{12} & C_{16} \\ C_{12} & C_{22} & C_{26} \\ C_{16} & C_{26} & C_{66} \end{array} \right] & \left[\begin{array}{ccc} B_{11} & B_{12} & B_{16} \\ B_{12} & B_{22} & B_{26} \\ B_{16} & B_{26} & B_{66} \end{array} \right] & \left[\begin{array}{ccc} D_{11} & D_{12} & D_{16} \\ D_{12} & D_{22} & D_{26} \\ D_{16} & D_{26} & D_{66} \end{array} \right] \\ \left[\begin{array}{ccc} E_{11} & E_{12} & E_{16} \\ E_{12} & E_{22} & E_{26} \\ E_{16} & E_{26} & E_{66} \end{array} \right] & \left[\begin{array}{ccc} D_{11} & D_{12} & D_{16} \\ D_{12} & D_{22} & D_{26} \\ D_{16} & D_{26} & D_{66} \end{array} \right] & \left[\begin{array}{ccc} F_{11} & F_{12} & F_{16} \\ F_{12} & F_{22} & F_{26} \\ F_{16} & F_{26} & F_{66} \end{array} \right] \end{array} \right] \left\{ \begin{array}{c} \left\{ \begin{array}{c} \varepsilon_x^0 \\ \varepsilon_y^0 \\ \gamma_{xy}^0 \end{array} \right\} \\ \left\{ \begin{array}{c} \chi_x^{e,b} \\ \chi_y^{e,b} \\ \chi_{xy}^{e,b} \end{array} \right\} \\ \left\{ \begin{array}{c} \chi_x^{e,s} \\ \chi_y^{e,s} \\ \chi_{xy}^{e,s} \end{array} \right\} \end{array} \right\}$$

$$\left[\begin{array}{c} Q_{yz} \\ Q_{xz} \end{array} \right] = \left[\begin{array}{cc} A_{44}^s & A_{45}^s \\ A_{45}^s & A_{55}^s \end{array} \right] \left\{ \begin{array}{c} \gamma_{yz}^s \\ \gamma_{xz}^s \end{array} \right\} \tag{2.18}$$

where

$$(A_{ij}, C_{ij}, E_{ij}, B_{ij}, D_{ij}, F_{ij}) = \sum_{k=1}^N \int_{z_k}^{z_{k+1}} \overline{Q}_{ij}(1, z, f, z^2, fz, f^2)\, dz \qquad i,j = 1,2,6$$

$$A_{ij}^s = \sum_{k=1}^N \int_{z_k}^{z_{k+1}} \overline{Q}_{ij} g^2\, dz \qquad i,j = 4,5 \tag{2.19}$$

The governing equations and boundary conditions can be obtained by minimizing the total potential energy with respect to u_0, v_0, w_b and w_s

$$\begin{aligned} \delta u_0: \quad & \frac{\partial N_x^e}{\partial x} + \frac{\partial N_{xy}^e}{\partial y} = \frac{\partial N_x^p}{\partial x} + \frac{\partial N_{xy}^p}{\partial y} \\ \delta v_0: \quad & \frac{\partial N_y^e}{\partial y} + \frac{\partial N_{xy}^e}{\partial x} = \frac{\partial N_y^p}{\partial y} + \frac{\partial N_{xy}^p}{\partial x} \\ \delta w_b: \quad & \frac{\partial^2 M_x^{e,b}}{\partial x^2} + \frac{\partial^2 M_y^{e,b}}{\partial y^2} + 2\frac{\partial^2 M_{xy}^{e,b}}{\partial x \partial y} + q = \frac{\partial^2 M_x^{p,b}}{\partial x^2} + \frac{\partial^2 M_y^{p,b}}{\partial y^2} + 2\frac{\partial^2 M_{xy}^{p,b}}{\partial x \partial y} \\ \delta w_s: \quad & \frac{\partial^2 M_x^{e,s}}{\partial x^2} + \frac{\partial^2 M_y^{e,s}}{\partial y^2} + 2\frac{\partial^2 M_{xy}^{e,s}}{\partial x \partial y} + q + \frac{\partial Q_{yz}^e}{\partial y} + \frac{\partial Q_{xz}^e}{\partial x} \\ & = \frac{\partial^2 M_x^{p,s}}{\partial x^2} + \frac{\partial^2 M_y^{p,s}}{\partial y^2} + 2\frac{\partial^2 M_{xy}^{p,s}}{\partial x \partial y} + \frac{\partial Q_{yz}^p}{\partial y} + \frac{\partial Q_{xz}^p}{\partial x} \end{aligned} \tag{2.20}$$

The boundary conditions for a simply supported plate are taken as below:
— at the edges $x = 0$ and $x = a$

$$v_0 = 0 \qquad w_b = 0 \qquad w_s = 0 \qquad M_x = 0 \qquad N_x = 0 \qquad \psi = 0 \tag{2.21}$$

— at the edges $y = 0$ and $y = b$

$$u_0 = 0 \qquad w_b = 0 \qquad w_s = 0 \qquad M_y = 0 \qquad N_y = 0 \qquad \psi = 0 \tag{2.22}$$

The Navier method is adopted for solution of the obtained governing equations using the following infinite Fourier series for independent variables

$$u_0 = \sum_{m=1,3,5}^{\infty} \sum_{n=1,3,5}^{\infty} u_{0,mn} \cos\frac{m\pi x}{a} \sin\frac{n\pi y}{b} \qquad v_0 = \sum_{m=1,3,5}^{\infty} \sum_{n=1,3,5}^{\infty} v_{0,mn} \sin\frac{m\pi x}{a} \cos\frac{n\pi y}{b}$$

$$w_b = \sum_{m=1,3,5}^{\infty} \sum_{n=1,3,5}^{\infty} w_{b,mn} \sin\frac{m\pi x}{a} \sin\frac{n\pi y}{b} \qquad w_s = \sum_{m=1,3,5}^{\infty} \sum_{n=1,3,5}^{\infty} w_{s,mn} \sin\frac{m\pi x}{a} \sin\frac{n\pi y}{b} \tag{2.23}$$

It can be easily verified that these expressions for displacements automatically satisfy the boundary conditions. Also the external load and the electrostatic potential can be approximated as the following double Fourier expansions

$$q_z = \sum_{m=1,3,5}^{\infty} \sum_{n=1,3,5}^{\infty} q_{z,mn} \sin \frac{m\pi x}{a} \sin \frac{n\pi y}{b}$$

$$\psi(x,y,z) = \sum_{m=1,3,5}^{\infty} \sum_{n=1,3,5}^{\infty} \psi_{mn}(z) \sin \frac{m\pi x}{a} \sin \frac{n\pi y}{b}$$

(2.24)

The electrostatic potential in the actuator layer is assumed to be linear through thickness of the PFRC layer (Shiyekar and Kant, 201)

$$\psi_{mn}(z) = \frac{V_t}{t_p} z - \frac{V_t h}{2t_p}$$

(2.25)

3. Numerical results and discussions

In this Section, several simply supported hybrid cross ply plates consisting of an elastic substrate with a piezoelectric layer of PFRC bonded to its top, subjected to mechanical and electric potential loadings are considered. The thickness of the PFRC actuator is $250 \, \mu$m and thickness of each orthotropic layer is 1 mm. Two different kinds of graphite/epoxy composites are considered for the substrate whose properties are as follows:
— material 1 (Malik and Ray, 2004)

$$[(E_1, E_2, G_{12}, G_{23}, G_{13}), \nu_{12}] = [(172.9, 6.916, 3.458, 1.383, 1.383) \, \text{GPa}, 0.25]$$

(3.1)

— material 2 (Kapuria and Achary, 2005)

$$[(E_1, E_2, G_{12}, G_{23}, G_{13}), \nu_{12}] = [(181, 10.3, 7.17, 7.17, 2.87) \, \text{GPa}, 0.28]$$

(3.2)

— and the material properties for the PFRC actuator are chosen as below (Malik and Ray, 2004)

$$\begin{aligned}
&C_{11} = 32.6 \, \text{GPa} && C_{12} = C_{21} = 4.3 \, \text{GPa} && C_{13} = C_{31} = 4.76 \, \text{GPa} \\
&C_{22} = C_{33} = 7.2 \, \text{GPa} && C_{23} = 3.85 \, \text{GPa} && C_{44} = 1.05 \, \text{GPa} \\
&C_{55} = C_{66} = 1.29 \, \text{GPa} && e_{31} = -6.76 \, \text{C/m}^2
\end{aligned}$$

(3.3)

Since PFRC consists of a number of piezoelectric fibers surrounded by a matrix material, the value of the effective piezoelectric constant in the direction of fibers e_{31} is significantly higher than other effective piezoelectric constants, and they can be neglected in comparison to e_{31} (Malik and Ray, 2004).

For convenience, the following normalized parameters are used for presenting the numerical results

$$\begin{aligned}
&\overline{\sigma}_x\left(\frac{a}{2}, \frac{b}{2}, \pm\frac{h}{2}\right) = \frac{\sigma_x}{q_0 S^2} && \overline{\tau}_{xy}\left(0, 0, \pm\frac{h}{2}\right) = \frac{\tau_{xy}}{q_0 S^2} \\
&\overline{u}\left(0, \frac{b}{2}, \pm\frac{h}{2}\right) = \frac{E_2}{q_0 S^3 h} u && \overline{w}\left(\frac{a}{2}, \frac{b}{2}, 0\right) = \frac{100 E_2}{q_0 S^4 h} w && S = \frac{a}{h}
\end{aligned}$$

(3.4)

3.1. Comparison of the results

Results of the presented formulation are compared with those of FEM (Ray and Malik, 2004), HOSNT12 (Shiyekar and Kant, 2011) and the exact solution by Malik and Ray (2004). Three laminate configurations are taken into account: three-layered symmetric $[0°/90°/0°]$, four-layered symmetric $[0°/90°/90°/0°]$ and four-layered anti-symmetric $[0°/90°/0°/90°]$. Material set 1, Eq. (3.1), is used for laminas in this Section. Mechanical and electric potential loadings are considered as the following cases:

- Case 1: doubly sinusoidal mechanical load ($q_0 = q_{z,11} = 40\,\text{N/m}^2$, downward) without applied voltage ($V = 0$).

- Case 2: doubly sinusoidal mechanical load ($q_0 = q_{z,11} = 40\,\text{N/m}^2$, downward) with doubly sinusoidal applied voltage at the top of PFRC ($V = +100\,\text{V}$).

- Case 3: doubly sinusoidal mechanical load ($q_0 = q_{z,11} = 40\,\text{N/m}^2$, downward) with doubly sinusoidal applied voltage at the top of PFRC ($V = -100\text{V}$).

Considering various thickness ratios ($S = 10, 20$ and 100) and various mechanical and electrical loads, normalized in-plane and transverse displacement ($\overline{u}, \overline{w}$) and the in-plane normal and shear stresses for the hybrid laminate $[0°/90°/0°]$ are listed in Table 1 and Table 2, respectively. It is observed that the obtained displacements and stresses are in good agreement with the exact solution, FEM and HOSNT12 results. In comparison to the exact solution, the presented theory, especially in the case of the thin plate ($S = 100$), is more accurate than FEM and HOSNT12. It should be noted that the present theory involves only four unknown functions, and compared to HOSNT12 with 12 unknown functions it can be concluded that this theory is very simple and accurate. The results indicate that effect of actuation is more effective for thick laminates than thin laminates. Also, the obtained displacements and stresses are more affected by electrical loads than the mechanical load.

Table 1. Normalized displacements of the square substrate $[0°/90°/0°]$

Theory	$S = 10$			$S = 20$			$S = 100$		
	$V = 0$	$V = 100$	$V = -100$	$V = 0$	$V = 100$	$V = -100$	$V = 0$	$V = 100$	$V = -100$
$\underline{u}(0, b/2, h/2)$									
Present	0.00671	−2.85984	2.87327	0.00635	−0.70527	0.71797	0.00623	−0.02216	0.03463
	[1.67]	[−8.95]	[−8.90]	[0.79]	[−2.43]	[−2.40]	[0.48]	[−0.63]	[0.08]
HOSNT12	0.00632	−3.11842	3.13105	0.00617	−0.71474	0.72709	0.00613	−0.02191	0.03416
	[−4.31]	[−0.72]	[−0.73]	[−2.05]	[−1.13]	[−1.16]	[−1.20]	[−4.33]	[−1.66]
FEM	0.00580	−2.82040	2.83190	0.00600	−0.69290	0.70490	0.00610	−0.02170	0.03390
	[−12.12]	[−10.21]	[−10.22]	[−4.76]	[−4.15]	[−4.17]	[−1.61]	[−2.69]	[−2.02]
Exact	0.00660	−3.14100	3.15420	0.00630	−0.72290	0.73560	0.00620	−0.02230	0.03460
$\underline{w}(a/b, b/2, 0)$									
Present	−0.57405	128.43902	−129.5871	−0.44833	30.05247	−30.9491	−0.40794	0.78957	−1.60545
	[−19.13]	[−3.56]	[−3.50]	[−7.86]	[−0.94]	[−1.15]	[−0.31]	[0.29]	[−0.03]
HOSNT12	−0.66806	129.05500	−130.3910	−0.47112	29.77240	−30.7146	−0.40432	0.77533	−1.58397
	[−5.91]	[−2.89]	[−2.91]	[−3.18]	[−1.86]	[−1.90]	[−1.12]	[−1.52]	[−1.31]
FEM	−0.65110	122.46000	−124.7001	−0.45710	28.28700	−29.2010	−0.40220	0.76320	−1.57760
	[−8.30]	[−7.86]	[−7.15]	[−6.06]	[−6.76]	[−6.74]	[−1.64]	[−3.06]	[−1.71]
Exact	−0.71000	132.90000	−134.3000	−0.48660	30.33700	−31.3100	−0.40890	0.78730	−1.60500

HOSNT12 – Shiyekar and Kant (2011), FEM – Ray and Malik (2004), exact – Malik and Ray (2004)

In the above and in all subsequent tables, values diven in square brackets denote percentage error calculated as follows: [% error]=(calculated – exact value)/(exact value)×100

The results of the in-plane and transverse displacement as well as the in-plane normal and shear stresses of the four-layered laminated composite $[0°/90°/90°/0°]$ are shown in Table 3. The obtained results using the presented theory are in good agreement with the exact solution and HOSNT12 results. In some cases, the present theory gives more accurate results compared to HOSNT12 for the laminate $[0°/90°/90°/0°]$; for example, for a moderately thick laminate $(S = 10)$ subjected to negative voltage, the maximum percent error in the present formulation and HOSNT12 are 3.88% and 16.30%, respectively. For a thin plate, $S = 100$, considering various electromechanical loads, the present results are more accurate than HOSNT12. The results of the in-plane and transverse displacement of the four-layered anti-symmetric laminated composite $[0°/90°/0°/90°]$ are listed in Table 4. Again, the results obtained by the presented formulation are in good agreement with the exact solution and FEM and HOSNT12 results.

Table 2. Normalized stresses of the square substrate $[0°/90°/0°]$

Theory	$S = 10$			$S = 20$			$S = 100$		
	$V = 0$	$V = 100$	$V = -100$	$V = 0$	$V = 100$	$V = -100$	$V = 0$	$V = 100$	$V = -100$
$\underline{\sigma}(a/b, b/2, \pm h/2)$									
Present	-0.53358	226.54470	-227.6118	-0.50494	55.8653	-56.8752	-0.49573	1.75183	-2.74541
	$[1.04]$	$[-8.93]$	$[-8.89]$	$[0.28]$	$[-2.45]$	$[-2.40]$	$[0.19]$	$[-0.17]$	$[-0.03]$
	0.55950	-75.6089	76.7279	0.52945	-18.0937	19.15266	0.51978	-0.21974	1.25934
	$[-0.50]$	$[5.50]$	$[5.40]$	$[-0.19]$	$[1.59]$	$[1.47]$	$[0.09]$	$[0.75]$	$[0.22]$
HOSNT12	-0.50746	247.54300	-248.5580	-0.49326	56.75720	-57.74370	-0.48872	1.73795	-2.71540
	$[-3.91]$	$[-0.49]$	$[-0.51]$	$[-2.03]$	$[-0.89]$	$[-0.91]$	$[-1.23]$	$[-0.97]$	$[-1.06]$
	0.55160	-70.76880	71.87200	0.52389	-17.4131	18.46090	0.51439	-0.20484	1.23362
	$[-1.90]$	$[-1.25]$	$[-1.26]$	$[-1.25]$	$[-2.23]$	$[-2.19]$	$[-0.94]$	$[-6.08]$	$[-1.83]$
FEM	-0.49150	235.46000	-236.4000	-0.50220	57.2670	-58.27600	-0.49410	1.74830	-2.73640
	$[-6.93]$	$[-5.35]$	$[-5.37]$	$[-0.26]$	$[0.00]$	$[0.00]$	$[-0.14]$	$[-0.38]$	$[-0.30]$
	0.52150	-71.56500	72.57000	0.53040	-17.0900	18.07400	0.51210	0.21060	1.24780
	$[-7.26]$	$[-0.14]$	$[-0.30]$	$[-0.02]$	$[-4.04]$	$[-4.24]$	$[-1.39]$	$[-196.56]$	$[-0.70]$
Exact	-0.52810	248.7600	-249.8200	-0.50350	57.26900	-58.27600	-0.49480	1.75490	-2.74450
	0.56230	-71.66600	72.79000	0.53050	-17.8100	18.87500	0.51930	-0.21810	1.25660
$\overline{\tau}_{xy}(0, 0, \pm h/2)$									
Present	0.02196	-7.35976	7.34675	0.02008	-1.79866	1.83883	0.01972	-0.05282	0.09268
	$[-15.86]$	$[-4.37]$	$[-5.18]$	$[-6.60]$	$[-1.28]$	$[-1.39]$	$[0.10]$	$[0.14]$	$[0.52]$
	-0.02196	4.62176	-4.66569	-0.02078	1.12370	-1.16527	-0.02040	0.02516	-0.06597
	$[-20.43]$	$[0.06]$	$[-0.17]$	$[-7.23]$	$[0.04]$	$[-0.22]$	$[-0.00]$	$[0.40]$	$[0.01]$
HOSNT12	0.02473	-7.56623	7.61569	0.02084	-1.79126	1.83293	0.01942	-0.05187	0.09071
	$[-5.24]$	$[-1.69]$	$[-1.71]$	$[-3.09]$	$[-1.69]$	$[-1.71]$	$[-1.43]$	$[-1.58]$	$[-1.62]$
	-0.02643	4.52824	-4.58109	-0.02191	1.10547	-1.14928	-0.02028	0.02462	-0.06518
	$[-4.25]$	$[-1.96]$	$[-1.99]$	$[-2.20]$	$[-1.58]$	$[-1.59]$	$[-0.59]$	$[-1.74]$	$[-1.18]$
FEM	0.02410	-7.00660	7.05470	0.02140	-1.81400	1.85650	0.01970	-0.05260	0.09150
	$[-7.66]$	$[-8.96]$	$[-8.95]$	$[-0.47]$	$[-0.44]$	$[-0.45]$	$[0.00]$	$[-0.19]$	$[-0.76]$
	-0.02510	4.24190	-4.29200	-0.02240	1.12320	-1.16790	-0.02040	0.02502	-0.06580
	$[-9.06]$	$[-8.16]$	$[-8.17]$	$[0.00]$	$[0.00]$	$[0.00]$	$[0.00]$	$[-0.16]$	$[-0.24]$
Exact	0.02610	-7.69600	7.74800	0.02150	-1.82200	1.86480	0.01970	-0.05270	0.09220
	-0.02760	4.61900	-4.67400	-0.02240	1.12320	-1.16790	-0.02040	0.02506	-0.06596

Table 3. Normalized displacements and stresses of the four-layered $[0°/90°/90°/0°]$ square laminate

Theory	V	S	$\overline{u}$ $(0, b/2, -h/2)$	$\overline{w}$ $(a/2, b/2, 0)$	$\overline{\sigma}_x$ $(a/2, b/2, -h/2)$	$\overline{\tau}_{xy}$ $(0, 0, -h/2)$
Present	100	10	0.4736 [2.53]	95.7006 [1.91]	−38.4517 [2.59]	3.0710 [4.39]
HOSNT12	100	10	0.5105 [10.52]	96.2234 [2.47]	−31.2141 [−16.72]	3.1209 [6.09]
Exact	100	10	0.4619	93.9010	−37.4800	2.9417
Present	100	20	0.1097 [0.82]	22.3460 [0.92]	−8.9204 [0.84]	0.7406 [1.59]
HOSNT12	100	20	0.1097 [0.83]	22.1061 [−0.16]	−8.1721 [−7.62]	0.7306 [0.22]
Exact	100	20	0.1088	22.1410	−8.8460	0.7290
Present	100	100	−0.0020 [0.75]	0.4811 [0.82]	0.1533 [−0.65]	0.0096 [1.05]
HOSNT12	100	100	−0.0021 [4.98]	0.4722 [−1.06]	0.1609 [4.25]	0.0093 [−1.82]
Exact	100	100	−0.0020	0.4772	0.1543	0.0095
			$(0, b/2, -h/2)$	$(a/2, b/2, 0)$	$(a/2, b/2, -h/2)$	$(0, 0, -h/2)$
Present	−100	10	−0.4879 [2.60]	−96.8654 [1.62]	39.5857 [2.64]	−3.1155 [4.02]
HOSNT12	−100	10	−0.5241 [10.23]	−97.6020 [2.40]	32.2792 [−16.30]	−3.1738 [5.96]
Exact	−100	10	−0.4755	−95.3180	38.5670	−2.9952
Present	−100	20	−0.1232 [0.90]	−23.2568 [0.57]	9.9951 [0.89]	−0.7827 [1.15]
HOSNT12	−100	20	−0.1230 [0.73]	−23.0727 [−0.23]	9.2209 [−6.93]	−0.7749 [0.14]
Exact	−100	20	−0.1221	−23.1250	9.9071	−0.7738
Present	−100	100	−0.0112 [0.28]	−1.3104 [0.11]	0.9023 [0.23]	−0.0509 [0.00]
HOSNT12	−100	100	−0.0111 [−0.99]	−1.2961 [−0.98]	0.8865 [−1.53]	−0.0505 [−0.77]
Exact	−100	100	−0.0112	−1.3089	0.9002	−0.0509

3.2. Parametric study

In this Section, a parametric study is carried out in order to investigate the effects of the thickness ratio, aspect ratio, number of layers, staking sequence and the amount of electrostatic loading on the displacements and stresses. A three-layered symmetric $[0°/90°/0°]$ laminate with a PFRC layer at the top is considered, and material set 2, Eq. (3.2), is used for laminas. Considering various aspect ratios, thickness ratios and applied electric voltages, the normalized in-plane and transverse displacements ($\overline{u}$ and $\overline{w}$) as well as the in-plane normal and shear stresses ($\overline{\sigma}_x$ and $\overline{\tau}_{xy}$) are collected in Table 5.

Figure 2 shows the effect of the aspect ratio a/b on the normalized central deflection $\overline{w}$. It can be seen that the maximum values of $\overline{w}$ are accrued for square laminates, and the deflections

Table 4. Normalized displacements of the four-layered $[0°/90°/0°/90°]$ square laminate

Theory	S = 10			S = 20			S = 100		
	V = 0	V = 100	V = −100	V = 0	V = 100	V = −100	V = 0	V = 100	V = −100
$\underline{u}(0, b/2, \pm h/2)$									
Present	0.00958	−3.37719	3.4004	0.00915	−0.83340	0.85171	0.00901	−0.02462	0.04265
	[−7.88]	[−33.90]	[−33.72]	[−2.65]	[−12.27]	[−12.07]	[0.08]	[−0.72]	[−0.35]
	−0.00638	0.60289	−0.6156	−0.00602	0.14208	−0.15412	−0.00590	−0.00004	−0.01178
	[1.26]	[−22.25]	[−21.97]	[0.33]	[−9.73]	[−9.02]	[0.00]	[−100.21]	[−0.17]
HOSNT12	0.00971	−4.73418	4.7536	0.00910	−0.92249	0.92948	0.00890	−0.02449	0.04227
	[−6.64]	[−7.34]	[−7.34]	[−3.16]	[−2.90]	[−4.05]	[−1.11]	[−1.24]	[−1.25]
	−0.00614	0.83670	−0.8489	−0.00593	0.15559	−0.16124	−0.00590	−0.00010	−0.01163
	[−2.60]	[7.89]	[7.71]	[−1.14]	[−1.15]	[−4.82]	[0.00]	[−100.56]	[−1.48]
FEM	0.00920	−4.53640	4.5643	0.00890	−0.85580	0.87350	0.00890	−0.02420	0.04190
	[−11.54]	[−11.21]	[−11.03]	[−5.32]	[−9.92]	[−9.83]	[−1.11]	[−2.42]	[−2.10]
	−0.00590	0.93350	−0.9452	−0.00590	0.16260	−0.17440	−0.00590	0.01790	−0.01150
	[−6.35]	[20.37]	[19.92]	[−1.67]	[3.30]	[2.95]	[0.00]	[−2.19]	[−2.54]
Exact	0.01040	−5.10940	5.1301	0.00940	−0.95000	0.96870	0.00900	−0.02480	0.04280
	−0.00630	0.77550	−0.7882	−0.00600	0.15740	−0.16940	−0.00590	−0.01180	0.01830
$\overline{w}(a/2, b/2, 0)$									
Present	−0.64860	133.12105	−134.6003	−0.51824	31.43049	−32.4669	−0.47637	0.78180	−1.73455
	[−9.12]	[−9.90]	[−9.76]	[−3.15]	[−2.94]	[−2.94]	[0.00]	[0.00]	[0.00]
HOSNT12	−0.65578	149.4720	−147.7830	−0.51616	31.94070	−32.3655	−0.47082	0.77082	−1.71292
	[−8.12]	[−0.86]	[−0.93]	[−3.54]	[−1.37]	[−3.25]	[−1.17]	[−1.40]	[−1.25]
FEM	−0.66430	131.9700	−131.6800	−0.51020	30.14200	−31.1630	−0.46940	0.75840	−1.69700
	[−6.92]	[−10.68]	[−11.72]	[−4.65]	[−6.92]	[−6.85]	[−1.47]	[−2.99]	[−2.17]
Exact	−0.71370	147.7500	−149.1700	−0.53510	32.38300	−33.4530	−0.47640	0.78180	−1.73460

are decreased by an increase in the aspect ratio. Also the effect of actuation is decreased by the growth of the aspect ratio. The effect of the thickness ratio a/h on the normalized stress $\overline{\sigma}_x$ with applied electric voltage $V = 100$ is presented in Fig. 3. It is observed that the effect of the aspect ratio is decreased by the growing thickness ratio.
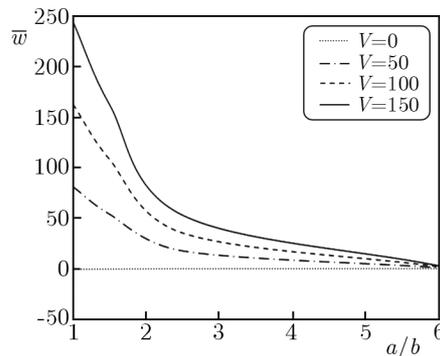

Fig. 2. Effect of the aspect ratio on the normalized deflection $\overline{w}$ of the symmetric substrate $[0°/90°/0°]$ considering various electric voltages ($S = 10$)

Some anti-symmetric square laminates $[0°/90°/\ldots]$ with various numbers of layers are considered and the transverse deflection $\overline{w}$ as well as the in-plane stress $\overline{\sigma}_x$ due to different amounts of electric voltage are obtained and listed in Table 6. It is seen that the values of $\overline{w}$ and $\overline{\sigma}_x$ are significantly decreased by an increase in the number of layers.

Table 5. Normalized displacements and stresses of the three-layered $[0°/90°/0°]$ square laminate

a/b	S	V	$\overline{u}(0, b/2, h/2)$	$\overline{w}(a/2, b/2, 0)$	$\overline{\sigma}_x(a/2, b/2, h/2)$	$\overline{\tau}_{xy}(0, 0, h/2)$
1	5	0	0.0095	−1.0124	−0.5383	0.04208
		50	−7.7428	366.6242	433.4841	−27.1126
		100	−15.4952	734.2608	867.5064	−54.2674
		150	−23.2476	1101.897	1301.5288	−81.4221
	10	0	0.0085	−0.6523	−0.4797	0.0375
		50	−1.9003	81.1370	106.3785	−6.6224
		100	−3.8092	162.9264	213.2367	−13.2823
		150	−5.7181	244.7158	320.0948	−19.9422
	100	0	0.0082	−0.5324	−0.4602	0.0359
		50	−0.0108	0.2517	0.6029	−0.0302
		100	−0.0298	1.0359	1.6660	−0.0964
		150	−0.0488	1.8201	2.7291	−0.1625
1.5	5	0	0.0063	−0.6524	−0.3641	0.0419
		50	−5.9044	243.1363	333.7615	−29.8249
		100	−11.8152	486.9251	667.8871	−59.6916
		150	−17.7260	730.7138	1002.0127	−89.5584
	10	0	0.005	−0.4290	−0.3252	0.0374
		50	−1.4521	53.9368	82.0600	−7.2974
		100	−2.9098	108.3027	164.4453	−14.6322
		150	−4.3676	162.6685	246.8305	−21.9670
	100	0	0.0054	−0.3543	−0.3122	0.0359
		50	−0.0091	0.1672	0.5078	−0.0370
		100	−0.0236	0.6889	1.3278	−0.1099
		150	−0.0381	1.2106	2.1479	−0.1828
2.5	5	0	0.0022	−0.2503	−0.1332	0.0241
		50	−3.2333	83.7739	185.0509	−23.3670
		100	−6.4688	167.7981	370.2351	−46.7641
		150	−9.7043	251.8123	555.4193	−70.1581
	10	0	0.0018	−0.1477	−0.1126	0.0203
		50	−0.7961	17.5660	45.5192	−5.7081
		100	−1.5942	35.2797	91.1509	−11.4366
		150	−2.3922	52.9935	136.7827	−17.1650
	100	0	0.0017	−0.1132	−0.1056	0.0191
		50	−0.0062	0.0528	0.3485	−0.0378
		100	−0.0142	0.2189	0.8026	−0.0968
		150	−0.0221	0.3850	1.2566	−0.1516

4. Conclusions

In this study, employing the four-variable refined plate theory, an analytical solution for cross-ply laminates integrated with a PFRC actuator subjected to mechanical and electrical loadings is presented. The governing equations are obtained using the principle of minimum potential energy and, in order to solve these equations, the Naveir solution has been utilized. The accuracy of the present method has been ascertained by comparing the obtained results with already published ones. It is observed that the present formulation gives more accurate results in predicting the
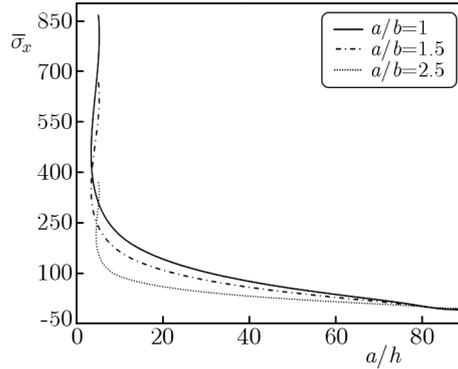
Fig. 3. Effect of the thickness ratio on the normalized stress $\overline{\sigma}_x$ of the symmetric substrate $[0°/90°/0°]$ considering various aspect ratios ($V = 100$)

Table 6. Normalized deflection $\overline{w}$ and stress $\overline{\sigma}_x$ of anti-symmetric cross-ply $[0°/90°/\ldots]$ square laminates ($S = 100$)

V	Number of layers					
	4		6		10	
	$\overline{w}(a/2,b/2,0)$	$\overline{\sigma}_x(a/2,b/2,h/2)$	$\overline{w}(a/2,b/2,0)$	$\overline{\sigma}_x(a/2,b/2,h/2)$	$\overline{w}(a/2,b/2,0)$	$\overline{\sigma}_x(a/2,b/2,h/2)$
0	-0.6102	-0.6461	-0.5774	-0.5782	-0.5627	-0.5380
50	0.1950	0.5759	-0.1049	0.1427	-0.3026	-0.1405
100	1.0003	1.7980	0.3677	0.8635	-0.0426	0.2571
150	1.8056	3.0202	0.8406	1.5843	0.2174	0.6546

displacements and stresses as compared to FEM-FOST and HOSNT12 formulations. It should be noted that the present theory involves only four unknown functions and, compared to HOSNT12 with 12 unknown functions, it can be concluded that this formulation is very simple and accurate.

The effects of the thickness ratio, aspect ratio, number of layers, staking sequence and amount of electrostatic loading on the displacements and stresses have been investigated and the obtained findings reported. It is observed that actuation is more effective in the case of thick laminates than in thin laminates, and the effect of actuation is decreased by increasing the aspect ratio a/b. As expected, the maximum values of normalized displacements and stresses are accrued in square laminates, and they are decreased by an increase in the number of layers.

References

1. Benachour A., Tahar H.D., Atmane H.A., Tounsi A., Ahmed M.S., 2011, A four variable refined plate theory for free vibrations of functionally graded plates with arbitrary gradient, *Composites Part B: Engineering*, **42**, 6, 1386-1394

2. Bouiadjra M.B., Houari M.S.A., Tounsi A., 2012, Thermal buckling of functionally graded plates according to a four-variable refined plate theory, *Journal of Thermal Stresses*, **35**, 8, 677-694

3. Hamidi A., Zidi M., Houari M.S.A., Tounsi A., 2014(??), A new four variable refined plate theory for bending response of functionally graded sandwich plates under thermomechanical loading, *Composites Part B: Engineering* (in press)

4. Kapuria S., Achary G.G.S., 2005, A coupled consistent third-order theory for hybrid piezoelectric plates, *Composite Structures*, **70**, 1, 120-133 15

5. Kapuria S., Dube G.P., Dumir P.C., Sengupta S., 1997, Levy-type piezothermoelastic solution for hybrid plate by using first-order shear deformation theory, *Composites Part B: Engineering*, **28**, 5/6, 535-546

6. KIM S.E., THAI H.T., LEE J., 2009a, A two variable refined plate theory for laminated composite plates, *Composite Structures*, **89**, 2, 197-205

7. KIM S.E., THAI H.T., LEE J., 2009b, Buckling analysis of plates using the two variable refined plate theory, *Thin-Walled Structures*, **47**, 4, 455-462

8. KUMAR A., CHAKRABORTY D., 2009, Effective properties of thermo-electro-mechanically coupled piezoelectric fiber reinforced composites, *Materials and Design*, **30**, 4, 1216-1222

9. MALLIK N., RAY M.C., 2003, Effective coefficients of piezoelectric fiber reinforced composites, *AIAA Journal*, **41**, 4, 704-710

10. MALLIK N., RAY M.C., 2004, Exact solutions for the analysis of piezoelectric fiber reinforced composites as distributed actuators for smart composite plates, *International Journal of Mechanics and Materials in Design*, **1**, 4, 347-364

11. MITCHELL J.A., REDDY J.N., 1995, A refined hybrid plate theory for composite laminates with piezoelectric laminate, *International Journal of Solids and Structures*, **3**, 16, 2345-2367

12. RAY M.C., BHATTACHARYA R., SAMANTA B., 1993, Exact solution for static analysis of intelligent structures, *AIAA Journal*, **31**, 9, 1684-1691

13. RAY M.C., MALLIK N., 2004, Finite element analysis of smart structures containing piezoelectric fiber reinforced composite actuator, *AIAA Journal*, **42**, 7, 1398-1405

14. REDDY J.N., 1999, On laminated composite plates with integrated sensors and actuators, *Engineering Structures*, **21**, 7, 568-593

15. SHIMPI R.P., 2002, Refined plate theory and its variants, *AIAA Journal*, **40**, 1, 137-146

16. SHIMPI R.P., PATEL H.G., 2006a, A two variable refined plate theory for orthotropic plate analysis, *International Journal of Solids and Structures*, **43**, 22/23, 6783-6799

17. SHIMPI R.P., PATEL H.G., 2006b, Free vibrations of plate using two variable refined plate theory, *Journal of Sound and Vibration*, **296**, 4/5, 979-999

18. SHIYEKAR S.M., KANT T., 2011, Higher order shear deformation effects on analysis of laminates with piezoelectric fiber reinforced composite actuators, *Composite Structures*, **93**, 12, 3252-3261

19. TAUCHERT T.R., 1992, Piezothermoelastic behavior of a laminated plate, *Journal of Thermal Stresses*, **15**, 1, 25-37

20. THAI H.T., KIM S.E., 2012, Analytical solution of a two variable refined plate theory for bending analysis of orthotropic Levy-type plates, *International Journal of Mechanical Sciences*, **54**, 1, 269-276

21. WANG B.T., ROGERS C.A., 1991, Laminate plate theory for spatially distributed induced strain actuators, *Journal of Composite Materials*, **25**, 4, 433-452